

Rapid Safety Assessment and Experimental Derivation of Damage Indexes for In-Service Glass Slabs

Chiara Bedon, Salvatore Noé

University of Trieste, Italy, chiara.bedon@dia.units.it

Abstract

The mechanical performance of pedestrian structures attracts the attention of several studies, especially with respect to unfavourable operational conditions or possible damage scenarios. In terms of vibrations, for example, specific customer comfort levels must be satisfied, depending on the class of use, the structural typology, the involved materials, in addition to basic safety requirements. A special consideration should be given to in-service systems that are possibly affected by degradation or even damage, and thus potentially unsafe for pedestrians. In this regard, the availability of standardized non-destructive protocols for a reliable and rapid structural safety assessment may result in efficient support for diagnostic analyses. In this paper, 3 different laminated glass (LG) modular units belonging to 2 different indoor in-service pedestrian systems located in Italy are investigated. Operational Modal Analysis (OMA) procedures and dynamic identification techniques are used to quantify the residual capacity of the examined systems, including damage and material degradation, based on a single triaxial Micro Electro-Mechanical System (MEMS) accelerometer. The experimentally derived performance indicators and calibrated mechanical parameters for the examined structural system are assessed towards traditional design procedures, and further quantified with the support of Finite Element (FE) numerical model updating. A comparative analysis is carried out to explore the structural performance and safety levels of in-service LG slabs in regards to vibration comfort, deflection control and stress analysis.

Keywords

Laminated glass (LG) pedestrian systems, Walk-induced vibrations, Glass fracture, Non-destructive field experiments, Finite Element (FE) numerical modelling, Damage measure, Residual capacity

Article Information

- Digital Object Identifier (DOI): [10.47982/cgc.8.403](https://doi.org/10.47982/cgc.8.403)
- This article is part of the Challenging Glass Conference Proceedings, [Volume 8](#), 2022, Belis, Bos & Louter (Eds.)
- Published by [Challenging Glass](#), on behalf of the author(s), at [Stichting OpenAccess Platforms](#)
- This article is licensed under a [Creative Commons Attribution 4.0 International License](#) (CC BY 4.0)
- Copyright © 2022 with the author(s)

1. Introduction

For civil engineering applications, the objective for a rapid structural safety assessment is to quickly inspect and evaluate the capacity of a given structural system, and to determine if the presence of any damage or issue is unsafe for customers (Baggio et al. 2007, MBIE 2014, etc.). In the framework of traditional buildings, two primary concerns need to be properly taken into account, namely (i) a quick evaluation of structural and non-structural components and (ii) the individuation of any visual sign of damage, and thus the possible detection of “unsafe” components. For “structural” components in reinforced concrete buildings, for example, visual damage will include cracks, failure evidence, spalling, etc., and typical conditions associated to risk. Field inspections, evenly supported by on-site measurements, can suggest rapid intervention or even a temporary monitoring process (Harirchian et al. 2020). Ad-hoc protocols may be required especially for severely damaged buildings with difficult accessibility or unsafe operational conditions (Stepinac et al. 2020).

In the field of laminated glass (LG) structural elements, similar needs can be rationally expected, especially characterized by a prevailing human-structure interaction. Typical examples are pedestrian LG systems under long-term effects and random walks (Bedon 2019a, Bedon 2020), or even balustrades (Kozłowski 2019). Some evidences of glass fracture can suggest urgent interventions (Bedon & Noè 2021). In some other cases, interlayer discolouring can be already representative of material deterioration (El-Sisi et al. 2020), but hardly quantifiable. Besides, intrinsic material properties and geometrical parameters suggest the need of dedicated assessment methods and performance indicators. Huang et al. (2018), for example, proposed a rapid safety assessment of curtain wall panels based on the remote vibration frequency measurement. Based on modal analysis results, it was shown that the first order inherent frequency is expected to decrease with an increase of sealant failure for linearly restrained glass panels. Similarly, the first order frequency amplitude scale of structural sealant was found to increase significantly with damage of silicon.

In the present study, the derivation of structural performance indicators for safety assessment of in-service LG pedestrian systems is explored. The attention is given to the use of single sensors in operational conditions (Step 1 in Figure 1), which are affected by several difficulties compared to laboratory experimental configurations.

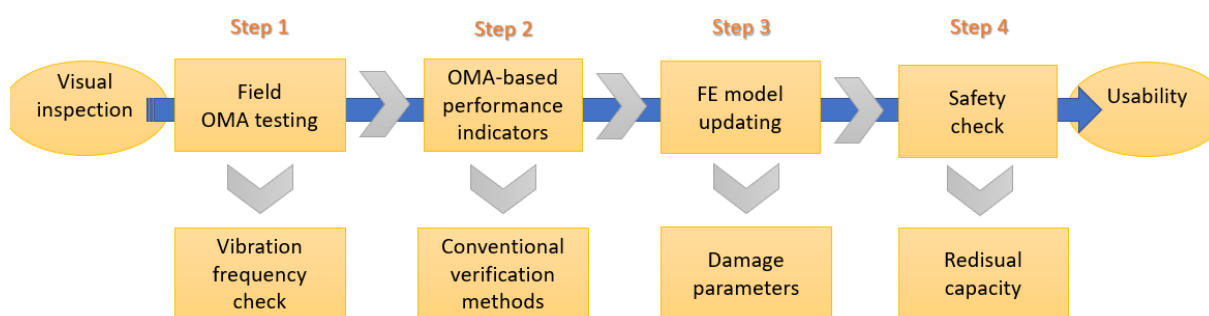


Fig. 1: Overall procedure for safety assessment of in-service LG pedestrian systems.

Three slab modules belonging to two different in-service LG pedestrian systems are taken into account in the present study. The first one, SM#1-LGU in the following, is representative of high-frequency system, while two others (SM#2-LGU and SM#3-LGF) are characterized by lower (but still not critical (ISO 10137:2007)) vibration frequency. Knowledge of actual frequency represents notoriously a powerful indicator, but still limited in interpretation as single parameter. The analysis and elaboration of basic on-site experimental data is thus proposed to derive possible quantification of damage

parameters (Step 2 in Figure 1). Further, additional discussion of experimental outcomes is proposed towards existing verification approaches for floors. Finally, a more detailed interpretation of experimental output is carried out with the support of Finite Element (FE) numerical models to characterize some basic equivalent material properties (Step 3 in Figure 1) and quantify long-term effects, thus residual capacity parameters for the existing LG system (Step 4 in Figure 1).

2. Methods

2.1. Operational Modal Analysis

Operational Modal Analysis (OMA) for structures and building component is known to represent a robust and efficient technique, able to offer a multitude of material and damage parameters. Major benefits are related by its possible application to structural components without the need of destructive interventions and service interruption (Dimarogonas 1996). The optimal setup definition is a critical step to capture relevant dynamic mechanical parameters. OMA is in fact generally very attractive because tests are cheap and fast, and they do not interfere with the normal use of the structure. Moreover, the identified modal parameters are representative of the actual behaviour of the structure in its operational conditions, since they refer to levels of vibration actually present in the structure and not to artificially generated vibrations (Limongelli et al. 2021).

When applied to exiting LG system, compared to other constructional systems, the typical size and mass parameters well apply to the imposed low-level vibrations. In (Bedon 2019a, Bedon 2020), for example, multiple MEMS accelerometers prototypes in (Bedon et al. 2018) have been used for diagnostic purposes in a suspension glass walkway (Figure 2 (a)). Fracture damage effects have been explored in (Bedon & Noè 2021). The effect of psychological discomfort on customers behaviour on glass structures, including LG pedestrian systems, has been addressed in (Bedon & Fasan 2019, Bedon & Mattei 2021). Following earlier experience, the present study aims at optimizing the interpretation of field experimental measurements in which a single sensor is used (Figure 2 (b)). This corresponds to a diagnostic investigation which is often subjected to operational limitations, as it is for emergency conditions, and does not allow the predefinition of special experimental protocols, or the use of multiple instruments, is not possible. As far as OMA techniques are applied to in-service LG pedestrian systems, typical outcomes take the form of an accurate vibration frequency estimate, which is inclusive of material properties, possible degradation phenomena, possible interaction with occupants.

Compared to analytical frequency calculations, more realistic estimates can be obtained with low-invasive, non-destructive field measures. According to classical theory, a beam-like LG system under free vibrations could be rationally assimilated to a slender Euler-Bernoulli beam with equivalent monolithic $b \times h$ section, and governed the reference differential equation of motion:

$$\frac{\partial^2}{\partial x^2} EJ(x) \left(\frac{\partial^2 v(x,t)}{\partial x^2} \right) + \rho A \frac{\partial^2 v(x,t)}{\partial t^2} = 0 \quad (1)$$

where $v(x,t)$ is the vertical displacement, at the abscissa x and time instant t ; E and ρ the modulus of elasticity and density of the material in use, J the second moment of area and A the cross-sectional area respectively.

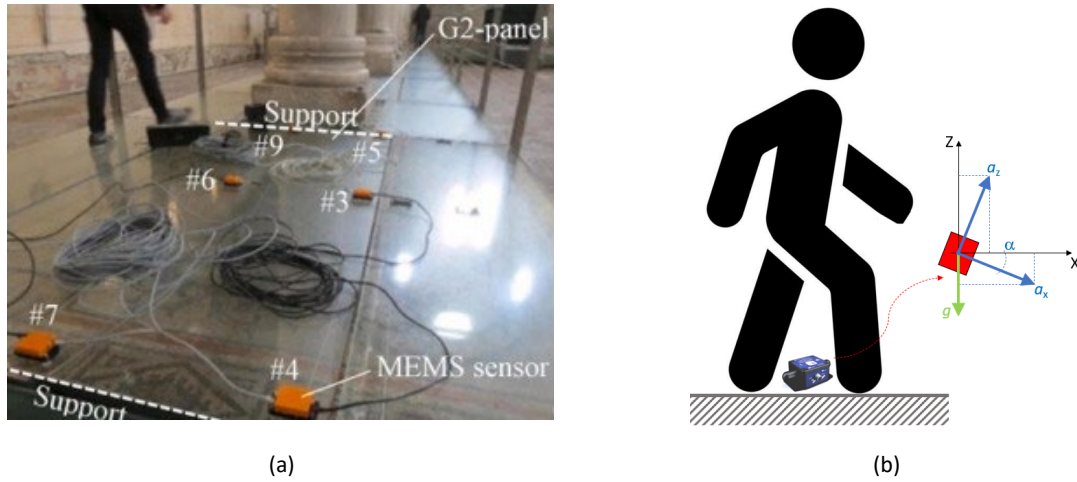


Fig. 2: Application of Operational Modal Analysis to in-service LG pedestrian systems: (a) past experimental study discussed in (Bedon 2019a) – figure reproduced with permission from Elsevier©, January 2022) and (b) schematic representation of present rapid field assessment, based on a single-MEMS setup.

As also shown in (Bedon 2019b), in presence of ideal restraints, its fundamental vibration frequency could be hence rationally calculated based on classical compact expressions, such as:

$$f_1 = \frac{\omega_1}{2\pi} = \frac{1}{2\pi} \sqrt{\frac{\beta_1^4 E}{12m}} h^3 \quad (2)$$

where β represents the well-known wavenumber given in Table 1.

Table 1. Reference wavenumbers β_n for beams with simple restraints and bending span L_0 .

Beam restraints	Mode order		
	1	2	3
Simply supports (S-S)	π/L_0	$2\pi/L_0$	$3\pi/L_0$
Clamps (C-C)	$4.73/L_0$	$7.8532/L_0$	$10.996/L_0$

For LG sections, assuming an equivalent monolithic glass thickness $h_{ef} = h$, it was shown in (Zemanova et al. 2019) that the “adjusted dynamic” effective thickness adapted from (Galuppi & Royer-Carfagni 2012) for modal analysis purposes is able to offer reliable frequency estimates, for double LG beams with different ideal restraints.

As such, the experimental frequency calculation is expected to offer a reference value which is comprised between the lower “abs” bound (weak connection of glass panels) and the upper “full” limit (rigid connection of glass panels).

$$f_{1,abs} \leq f_1 \leq f_{1,full} \quad (3)$$

However, intrinsic limits of Equation (2) are represented by multiple aspects, such as (i) the lack of occupant’s mass (which is relevant for LG pedestrian systems); (ii) the sensitivity of viscoelastic interlayer stiffness to ageing and time loading (Andreozzi et al. 2015, Zemanova et al. 2019; El-Sisi et al. 2020) or even delamination (Bedon 2019b); (iii) the possible effect of local phenomena due to non-ideal restraints (Bedon et al. 2020).

2.2. Finite Element model updating

For SHM applications, the use of Finite Element (FE) numerical methods is known to represent a strategic step in support of mechanical analysis of unknown parameters of the structural systems under investigation. A multitude of practical examples can be found in the literature especially for bridge structures or historical buildings affected by structural damage after earthquakes or other unfavourable operational conditions (Limongelli et al. 2021).

In the present study, the attention is focused on the analysis of damage and degradation phenomena for LG pedestrian systems, and thus in finding equivalent mechanical properties for constituent materials subjected to long-term phenomena, uncontrolled ambient condition, and even glass fracture (Bedon & Noè 2021). Such an approach, as shown, requires detailed knowledge of geometrical properties for structural and non-structural components, given that even supports and restraints can severely affect the overall dynamic response and mechanical parameters of a given glass component (Bedon et al. 2020).

For the present fitting procedure, a reference performance indicator is represented by the experimentally derived vibration frequency of the examined systems, which is known to represent a first strategic parameter for SHM purposes and damage detection (Dimarogonas 1996). In this regard, it is worth to note that LG pedestrian systems are often characterized by the use of multiple modular units, in which basic geometrical and mechanical features are repeated several times to cover wide surfaces, and this is a major difference from other pedestrian systems in constructions. Accordingly, different effects can be also expected from pedestrians and occupants (Busca et al. 2014, Bedon 2020).

2.3. Verification check and residual capacity measure

A final step to quantify damage and / or degradation of mechanical properties should take into account the application of conventional verification procedures for stress (at the Ultimate Limit State – ULS) and deformation indicators (at the Serviceability Limit State – SLS) of LG structural systems. Knowledge of actual residual capacity of a structural system in operational conditions is crucial for safety purposes. In this study, following Figure 1, the procedure is carried out in accordance with CNR-DT 210/2013 provisions.

3. Selected in-service LG pedestrian systems

For the present study, three different in-service LG slabs were taken into account. A single occupant (adult volunteer, $M = 80$ kg) was invited to take part in the experimental measurements.

3.1. Geometrical and mechanical properties

All the samples are characterized by a beam-like flexural behaviour under sustained occupants (2 linearly restrained edges), and a triple LG section. All the samples, moreover, are part of pedestrian systems located in Friuli Venezia Giulia region (Italy), and installed to take place in two historical churches, where they are used to allow visibility of underground Roman age manufactures (Figure 3).

The first one, herein called SM#1-LGU, is located in San Giorgio di Nogaro (UD). At the time of the experimental analysis (December 2020), the typical modular unit was characterized by 8 / 10 / 8 mm thick, fully tempered (FT) glass layers to compose the resisting LG section, with 0.76 mm thick PVB bonding layers. The original pedestrian system, ≈ 15 years apart from the on-site installation, has been retrofitted during Spring 2021 and replaced structural components with identical properties (Figure 3

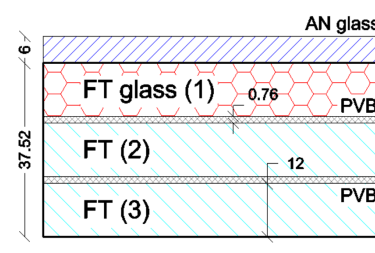
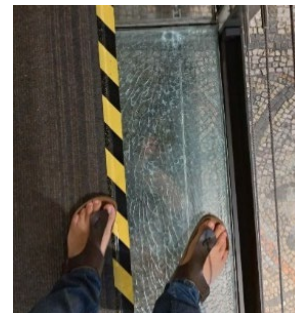
(a). The total size is $L= 2.80$ m in length by $B= 0.51$ m in width, and hollow box steel frame members (60 mm \times 100 mm in section, 5 mm in thickness) are used to realize a linear support along the maximum edges. The connection takes advantage of interposed 5 mm thick and 20 mm wide rubber tapes. Such a geometrical configuration resulted by specific site features at the time of the original design planning (Figure 3 (a)), and resulted in relatively stiff LG panels with a short bending span B .



(a)



(b)



(c)

Fig. 3: Overview of examined LG pedestrian systems: (a) SM#1-LGU layout (pictures taken during retrofit interventions, Courtesy of Seretti Vetroarchitettura), (b) top view of SM#2-LGU modular unit (reproduced from (Bedon & Noè 2021) under the terms and conditions of CC-BY license) and (c) glass failure detail for SM#3-LGF panel.

The second and third samples are located in Aquileia (UD), and belong to the suspension glass walkway investigated in (Bedon 2019a, Bedon 2020). Each modular unit has total dimension of $B= 1.35$ m \times $L= 2.65$ m (Figure 3 (b)). The slab module consists of a triple section composed of FT glass layers (3 mm \times 12 mm in thickness) and interposed PVB foils (0.76 mm their thickness). An additional protective layer made of annealed (AN) glass (6 mm in thickness) is positioned on the LG top surface. The mechanical

interaction between LG and the top AN layer is ensured by contact only. The tested modular units are linearly supported along the short edges. To limit large bending deformations under walking occupants, two pairs of pre-stressed tendons composed of AISI 316 steel are used (10 mm the nominal diameter). Their mechanical interaction with the bottom surface of LG is offered by two unilateral mechanical mid-span point supports only. The difference of two selected modules was represented by the presence of intact glass layers (SM#2-LGU) for the LG + AN sample, or by the presence of one fractured glass layer for the LG section (SM#3-LGF). To note that the top LG layer was fractured during maintenance operations, and a carpet was temporarily used to cover cracks, before replacing the LG + AN module (Figure 3 (c)).

Some further properties of the examined LG modules are summarized in Table 2, where the structural mass and the mass ratio R_M :

$$R_M = \frac{M_{structure}}{M_{occupant}} \quad (4)$$

are also presented. Finally, the geometric slenderness in Table 2 is calculated as:

$$\lambda = \frac{L_{eff}}{\bar{\rho}} \quad (5)$$

on the base of the effective bending span L_{eff} . The radius of gyration of interest for the flexural performance of each system under vertical pedestrian loads is given by:

$$\bar{\rho} = \sqrt{\frac{J}{A}} \quad (6)$$

To note that glass layers only were taken into account for preliminary calculations reported in Table 2.

Table 2: Summary of geometrical features for the examined LG pedestrian modules.

Specimen	Dimensions [m]	Span [m]	Thickness [mm]	Section	Mass [kg]	R_M	λ
SM#1-LGU	0.51 x 2.8	0.51	27.52	8/10/8 + 0.76 PVB	93	1.16	68
SM#2-LGU	1.35 x 2.65	2.65	37.52 + 6	12/12/12 + 0.76 PVB + AN cover	320	4	245
SM#3-LGF	1.35 x 2.65	2.65	37.52 + 6	12/12/12 + 0.76 PVB + AN cover	320	4	245

The mass ratio R_M , more in detail, is of interest for the assessment of human-structure interaction phenomena. Compared to other constructional typologies, for LG pedestrian solutions it is typically small (Bedon 2020). It can be seen in Table 2 that the SM#1-LGU module, for example, is characterized by structural mass (glass section) in the same order of the involved occupant, and thus this may result in higher resonance effects.

On the other side, see Table 2, the geometric slenderness of SM#1-LGU module is relatively small compared to SM#2-LGU and SM#3-LGF solutions, based on the short bending span. The geometric slenderness in Table 2 from Equation (5), however, does not account for the modification of shear stiffness of the interlayers in use, and thus is representative of a lower limit value only.

Under dynamic loads, it is thus expected that multiple mechanical and geometrical aspects can mutually affect the final performance of similar systems.

3.2. Preliminary visual inspection

All the samples were subjected to preliminary visual inspection to detect possible anomalies, visible damage and other possible issues. For the present investigation, no visible damage was observed for SM#1-LGU and SM#2-LGU samples, with regard to glass panels or restraints. PVB discolouring was perceived in the bonding layers, and this still represent a signal of deterioration (El-Sisi et al. 2020). Visible and rather uniform fracture in the top glass layer was recorded for SM#3-LGF module, as schematized in Figure 3 (c).

A common feature of all the samples was characterized by unfavourable operational conditions, given the presence of non-controlled humidity and temperature (Bedon 2019a), and their installation carried out several years ago (≈ 15 years their average age), compared to the typical warranty period of most LG manufacturers (El-Sisi et al. 2020). To note that the experimental measures were collected for the SM#1-LGU sample under maintenance interventions (Figure 3 (a)), while the experimental investigation for SM#2-LGU and SM#3-LGF samples was carried out under normal operational conditions.

3.3. Finite Element numerical modelling

The numerical analysis of selected slab modules was carried out in ABAQUS (Simulia 2021). Element features, mesh size and features and material properties were calibrated to optimize the computational efficiency of simulations, as well as by taking into account past efforts (Bedon 2019a, Bedon & Noè 2021). As a basic step towards the on-site experimental output, a linear modal frequency analysis procedure was preliminary taken into account, so as to fit the unknown material properties and degradation features towards the experimentally measured vibration frequency of the selected samples. Figure 4 shows a typical example of assembled modular units.

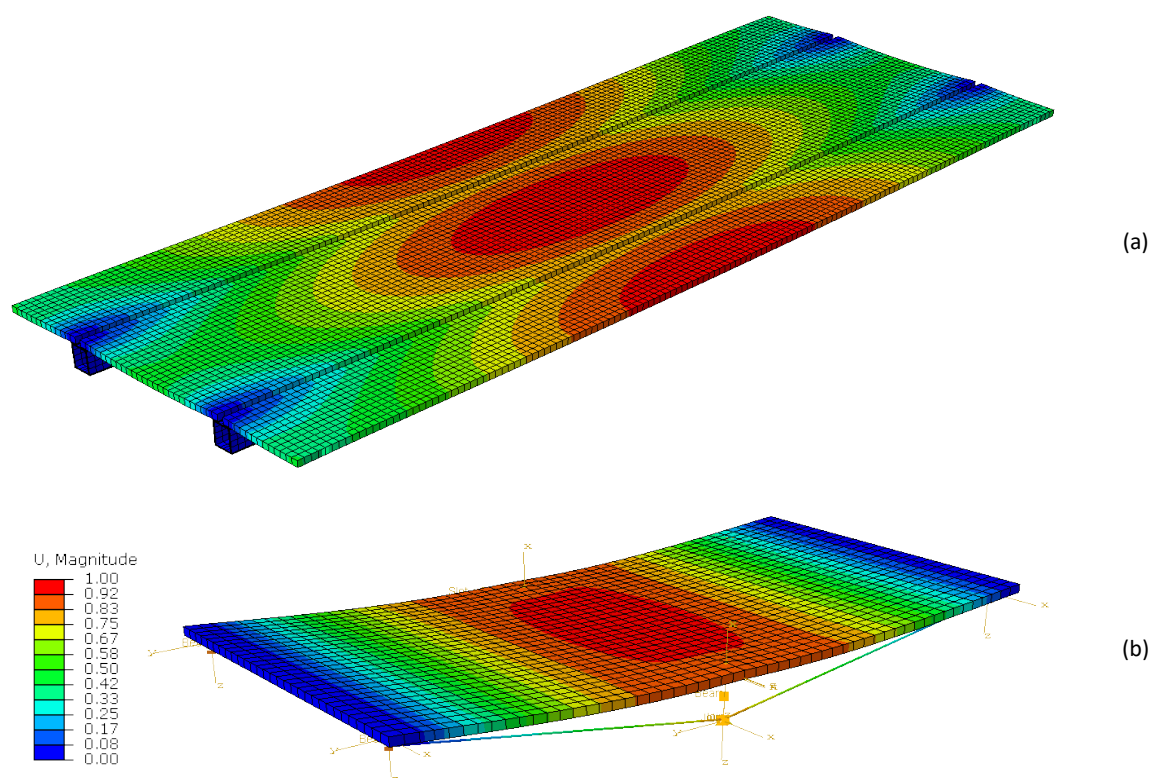


Fig. 4: Qualitative frequency response of (a) SM#1-LGU modular unit and (b) SM#2-, SM#3 systems (ABAQUS).

4. Experimental results and diagnostic investigation

4.1. Frequency analysis under random walks

All the experimental measurements were performed using a single triaxial Micro Electro-Mechanical System (MEMS) accelerometer (Bedon et al. 2018). Output-only test data were collected under the effects of normal walks or in-place jumps. The overall experimental analysis included different configurations and test repetitions on the selected modules, with up to 9 repetitions for SM#1-LGU, 14 repetitions for SM#2-LGU and 18 for SM#3-LGF respectively. Due to the limited size of each slab module, the on-site experimental configurations included linear walking paths along the mid-line of each panel. In-place jumps were also carried out at the centre of panels. A single MEMS sensor was in fact used to capture the acceleration time histories of interest. The typical record was characterized by a maximum duration of ≈ 2 min.

Figure 5 shows selected examples of FFT signals from vertical accelerations. It can be easily perceived a markedly different vibration response of examined modules, with relatively high variation of fundamental vibration frequency. Compared to existing design standards to prevent severe vibration issues in pedestrian systems, it is possible to see that FFT peaks denoting the presence of vibration modes are significantly higher than the recommended minimum value of 5 Hz (Bedon & Fasan 2019). Besides, it is worth to note that the mechanical and geometrical properties of typical LG slabs are relatively different from other construction typologies, and thus result in higher sensitivity to walking induced effects.

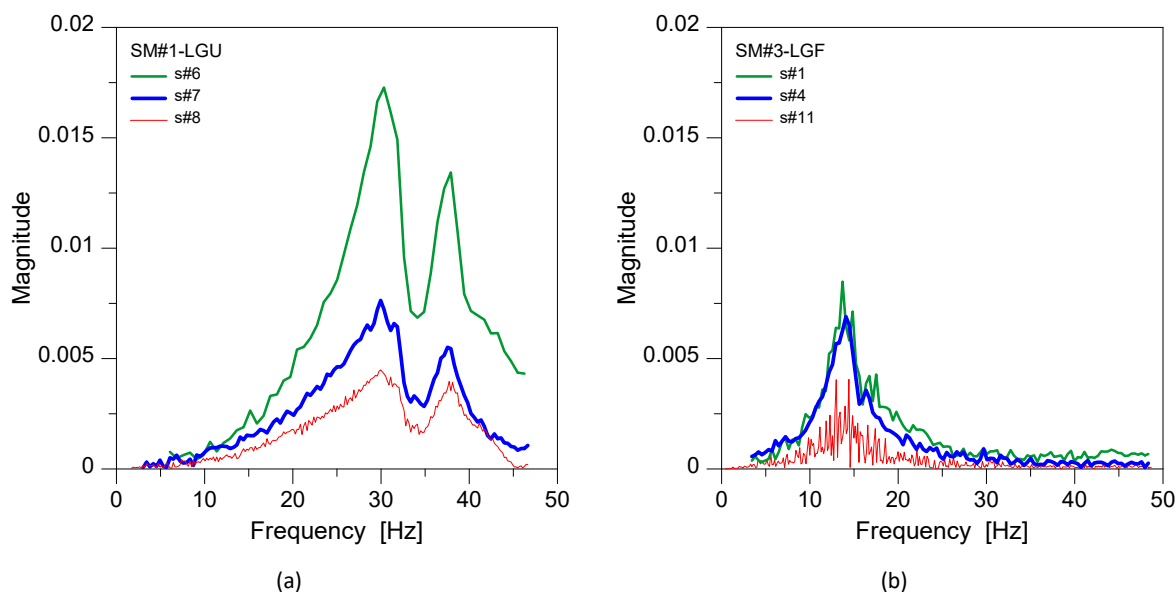


Fig. 5: Frequency domain response of the examined systems: example of selected experimental signals for the (a) SM#1-LGU and (b) SM#3-LGF modules.

The experimental vibration frequency of the examined systems was measured in 30 Hz (± 0.39) for SM#1-LGU system. For SM#2-LGU and SM#3-LGF slabs with similar geometrical and mechanical properties, but different damage magnitude, the experimental investigation resulted in 15.05 Hz (± 0.2) and 13.8 Hz (± 0.21), thus up to -8.3% vibration frequency decrease, due to glass fracture (Bedon & Noè 2021). Often, no interventions and verifications are required for traditional slabs and floors with fundamental frequency higher than 5-8 Hz (ISO 10137:2007). On the other side, it was shown also in (Bedon & Fasan 2019) that existing reference indicators and comfort assessment procedures cannot

directly applied to LG slabs with specific dynamic parameters and human-structure interaction phenomena. Knowledge of field vibration frequency is certainly a rapid and reliable parameter, but necessarily needs a comparative term to quantify modifications of mechanical features in time.

In this regard, an intermittent field monitoring program for in-service LG structures to characterize the actual vibration frequency of a given system (from “Time 0” of original installation apart), would certainly facilitate any kind of diagnostic analysis and maintenance plan, and give a concise measure of any kind of modification in the involved structural parameters.

4.2. Damping

FFT signals as in Figure 5 are of utmost importance for simplified damping estimates (Clough & Penzien 1993). A number of studies have demonstrated that damping has greater sensitivity for characterizing damage than natural frequencies and mode shapes in various applications, but damping-based damage identification is still a research direction ‘in progress’ and is not yet well resolved (Cao et al. 2017). Among others, the half-power bandwidth method is the most representative and widely used approach, due to simplicity in implementation. Accordingly, while damping in LG systems can be affected by several parameters, the analysis of experimental signals in the frequency domain gives:

$$\xi = \frac{1}{2Q} \quad (7)$$

with:

$$Q = \frac{f_{max}}{f_{m,2} - f_{m,1}} \quad (8)$$

where the values in Equation (8) are calculated as in the schematic drawing of Figure 6. f_{max} is the resonant frequency and $f_{m,1}$, $f_{m,2}$ the frequencies at the left-hand and right-hand sides of f_{max} respectively, with the amplitude of $f_{m,1}$ and $f_{m,2}$ being calculated as $1/(2^{0.5})$ times that of f_{max} . For the presently examined in-service systems, the average damping was quantified in 6.78% for SM#1-LGU, 7.25% for SM#2-LGU and 8.95% for SM#3-LGF module. The so-calculated damping values reveal a rather uniform value for SM#1-LGU and SM#2-LGU systems, and a relatively higher damping term for the SM#3-LGF affected by partial glass fracture.

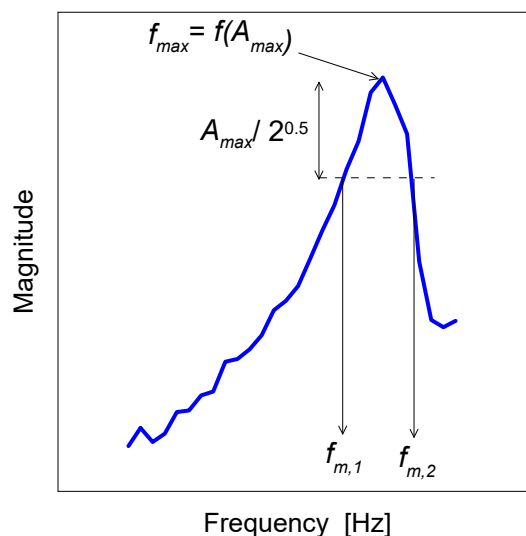


Fig. 6: Rapid damping computation based on classical FFT-based classical half-power bandwidth method.

4.3. Vibration assessment based existing conventional approaches

The analysis of structural performances was carried out, based on collected experimental output, in terms of maximum vertical acceleration, peak-to-peak acceleration, RMS acceleration (Equation (9)) or rolling RMS acceleration, based on limited intervals for each signal (Equation (10)):

$$a_{RMS} = \sqrt{\frac{1}{T} \int_0^T a(t)^2 dt} \quad (9)$$

$$a_{RMS}(t) = \sqrt{\frac{\sum_0^n a(t)^2}{n}} \quad (10)$$

with T (in seconds) the total duration of each signal, and n the number of recorded data in a time interval of 0.5 seconds.

Finally, the rolling RMS velocity was also taken into account, since representative of robust feedback for floor vibrations:

$$v_{RMS}(t) = \sqrt{\frac{\sum_0^n v(t)^2}{n}} \quad (11)$$

A qualitative example can be seen in Figure 7, as obtained from a single footfall of the involved volunteer (SM#3-LGF system).

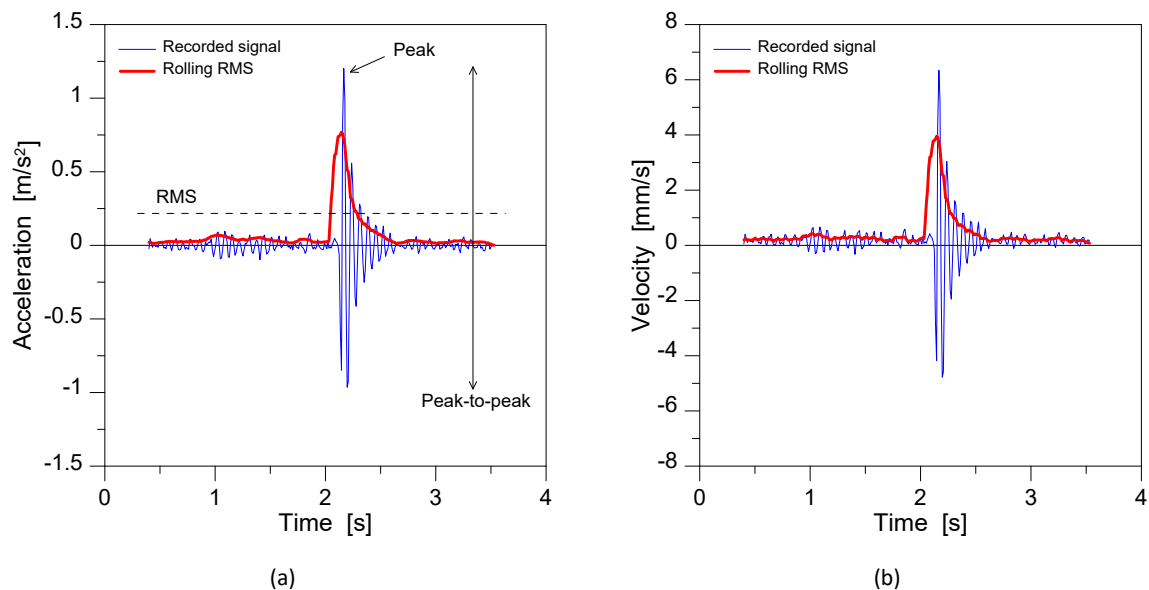


Fig. 7: Qualitative example of typical (a) acceleration and (b) velocity experimental signal due to a single footfall of the involved volunteer.

Multiple design standards are available in support of the vibration serviceability assessment of pedestrian systems. In the present study, the reference limit values and indicators were derived from ISO document (ISO 10137:2007) and compared to available signals. As far as the acceleration parameters are taken into account, typical results can be found in Figure 8, where it is possible to see that all the three modules are associated to vertical acceleration peaks exceeding the limit recommended values for “indoor footbridges”, as it could be considered for the examined systems.

RMS acceleration values from the experiments are also reported in Figure 8, for comparison with the ISO baseline curve. According to ISO 10137:2007, the limit values for RMS acceleration should be in fact calculated on the base of input vibration frequency of the system and its destination.

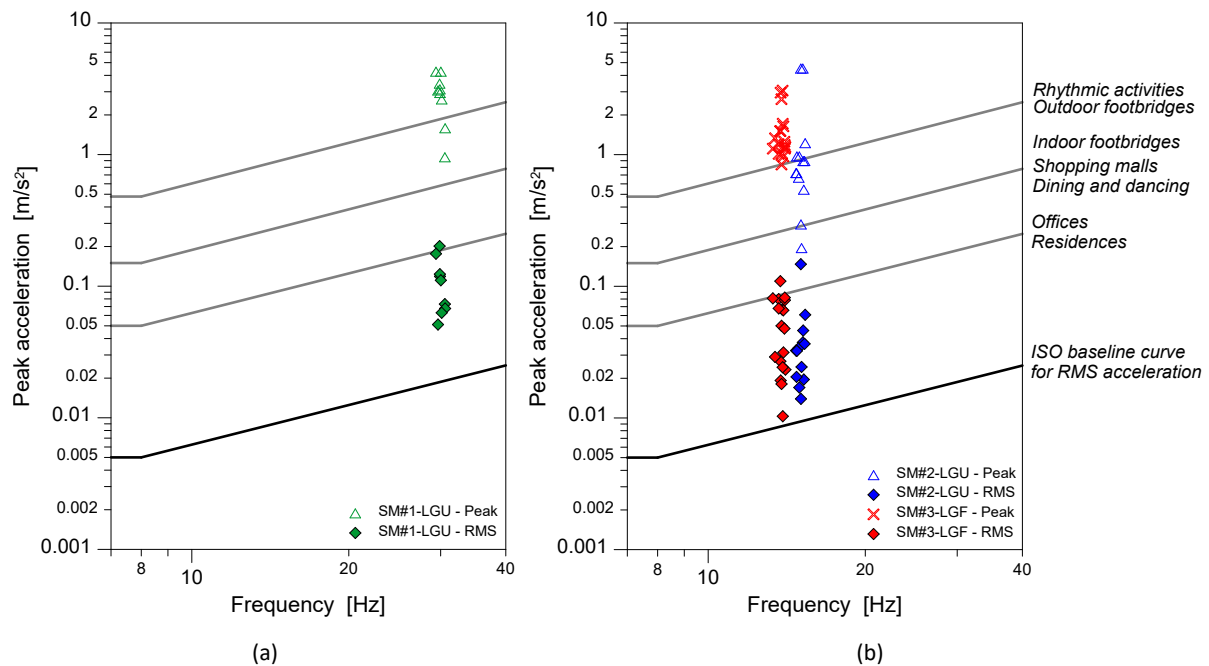


Fig. 8: Reference ISO 10137:2007 acceleration curves for RMS and peak acceleration on floors. Application of recommended limits to (a) SM#1-LGU and (b) SM#2-LGU, SM#3-LGF modular units.

Typical reference values are reported in Table 3. Based on Figure 8, the ISO baseline values are in the order of 0.02 m/s² for SM#1-LGU system, 0.007 m/s² for SM#2-LGU and 0.006 m/s² for SG#3-LGF module respectively. The experimental investigation resulted in average RMS accelerations in the order of 0.109 m/s² for SM#1-LGU, 0.040 m/s² for SM#2-LGU and 0.051 m/s² for SM#3-LGF respectively. The corresponding experimentally derived MF (average) values are proposed in Table 3, for comparison with recommended values. As shown, calculated MF values for SM#1-LGU and SM#2-LGU systems are comparable, less than 6. A relatively high calculated MF value can be observed for the SM#3-LGF system with glass fracture. Especially compared to the uncracked SM#3-LGU system with identical size and section features, this is an additional parameter representative of possible damage.

Table 3: Reference multiplying factors (MF) and experimentally derived MF values for continuous and intermittent vibrations, based on ISO 10137:2007.

Floor	Time	Recommended limit MF	Experimentally calculated MF (average)
Critical working area	Day & Night	1	
Residential	Day	2 to 4	
	Night	1.4	0.109 / 0.02 = 5.47 for SM#1-LGU
Quite office, Open plan	Day & Night	2	0.040 / 0.007 = 5.71 for SM#2-LGU
General office	Day & Night	4	0.051 / 0.006 = 8.50 for SM#3-LGF
Workshop	Day & Night	8	

For vibration assessment purposes, the rolling RMS velocity of a given pedestrian system is also known to represent an efficient performance indicator.

Based on (Sedlacek et al. 2006, Feldmann et al. 2009), for example, limit values and ranges are given to detect possible critical configurations, depending on the dynamic response of floors and on the destination of the structural system. A summary of recommended values is summarized in Table 4.

Table 4: Classification of floor response based on measured RMS velocity (Sedlacek et al. 2006, Feldmann et al. 2009).
Green= recommended; orange= critical; red= not recommended

Class	Lower limit [mm/s]	Upper limit [mm/s]	Critical workplace	Health, Education	Residential, Office, Meeting, Retail, Hotel	Industrial, Sport	
A	0	0.1					
B	0.1	0.2					
C	0.2	0.8					
D	0.8	3.2					
E	3.2	12.8			**	**	
F	12.8	51.2					

For the present study, the average peak of rolling RMS velocity from Equation (6) was calculated in 7.11 mm/s for SM#1-LGU system, 3.61 mm/s for SM#2-LGU module and 4.44 mm/s for SM#3-LGF sample respectively. In accordance with Table 4, it can be seen that all the examined systems find place in class “E” and may result in preferably suitable vibration performances for industrial or sport applications only. Such an outcome can suggest a high sensitivity of case-study solutions to walk induced effects.

4.4. Structural assessment based on trend of field performance indicators

AS far as OMA techniques are particularly simple to apply in systems under normal operational conditions, the critical stage is represented by collection of a sufficient number of signals for data interpretation and diagnostic analysis. In the present study, the total set of experimental signals was further elaborated to find possible correlation of structural performance indicators and actual damage state of the examined systems. Typical comparative results can be seen in Figure 9.

In Figure 9 (a), experimental frequency values are reported as a function of vertical acceleration peaks. The average experimental frequency values with standard deviation are also shown for the three samples. A relatively uniform frequency trend can be noticed for each one of them, with relatively small standard deviation for each system, as far as they are subjected to different impulse. Multiple signals for a given module can thus possibly suggest the consistency of experimental records, or even the presence of possible issues. In this regard, it is worth to note the different frequency response of SM#2-LGU and SM#3-LGF modules. For similar units, such a trend can suggest possible mechanical defects as it is for SM#2-LGU and SM#3-LGF slabs, given that the experimental investigation revealed up to -8.3% vibration frequency decrease, due to glass fracture.

In Figure 9 (b), the vertical acceleration peak is shown as a function of the rolling RMS acceleration value, for all the collected signals. It can be noticed a rather linear correlation for all the available experimental signals, as also suggested by the linear regression method and the *R*-square correlation

coefficient. Worth to note, in this sense, that a limited modification can be observed for the three samples. All the trends are characterized by R -square value close to the unit. In any case, the SM#3-LGF system with glass fracture has the lowest correlation of dynamic performance indicators. While such a comparison should be extended to multiple slab units with different damage scenarios, such a correlation could be a parameter of practical feedback for diagnostic purposes. Similarly, a correlation coefficient in the order of 1 could represent an optimum for safety check assessment.

In Figure 9 (c), finally, the RMS acceleration value is indeed shown as a function of the vertical acceleration peak, where the RMS value takes into account the total duration of experimental signals, rather than progressive time intervals as for the rolling RMS acceleration value. In this context, major scatter from the linear regression method can be noticed for the SM#3-LGF sample affected by glass fracture, which has a relatively low R -square correlation coefficient but also a substantially different trend, compared to SM#1-LGU and SM#2-LGU samples. Also in this case, such a kind of correlation parameters and trends could reveal useful information for rapid diagnostic analyses.

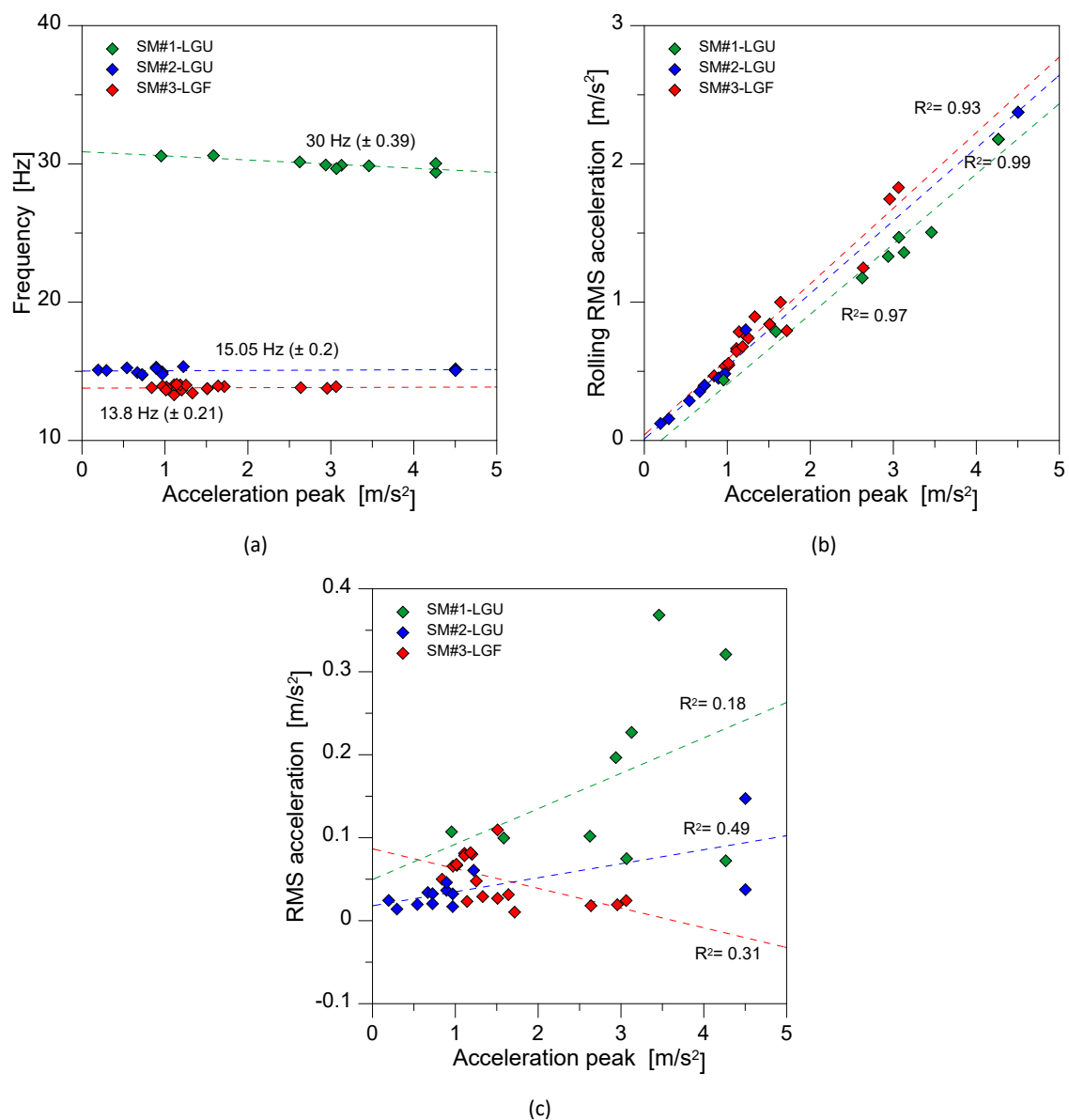


Fig. 9: Correlation analysis of experimental performance indicators for the examined slab units: (a) vibration frequency as a function of the vertical acceleration peak; (b) rolling RMS acceleration as a function of the vertical acceleration peak and (c) RMS acceleration as a function of the vertical acceleration peak.

4.5. Material characterization based on Finite Element updating

Apart from field experimental measures and derived performance indicators on the side of field structural performance, an advanced level of safety assessment as in Figure 1 necessarily requires the use of refined FE numerical models able to capture the geometrical and mechanical features of the real systems object of study.

In the present study, based on field observations, the attention was focused on model updating in terms of equivalent shear stiffness for the bonding PVB foils (all systems) and on the calibration of the equivalent E modulus for the fractured glass layer (SM#3-LGF system).

Typical comparative results are proposed in Figure 10.

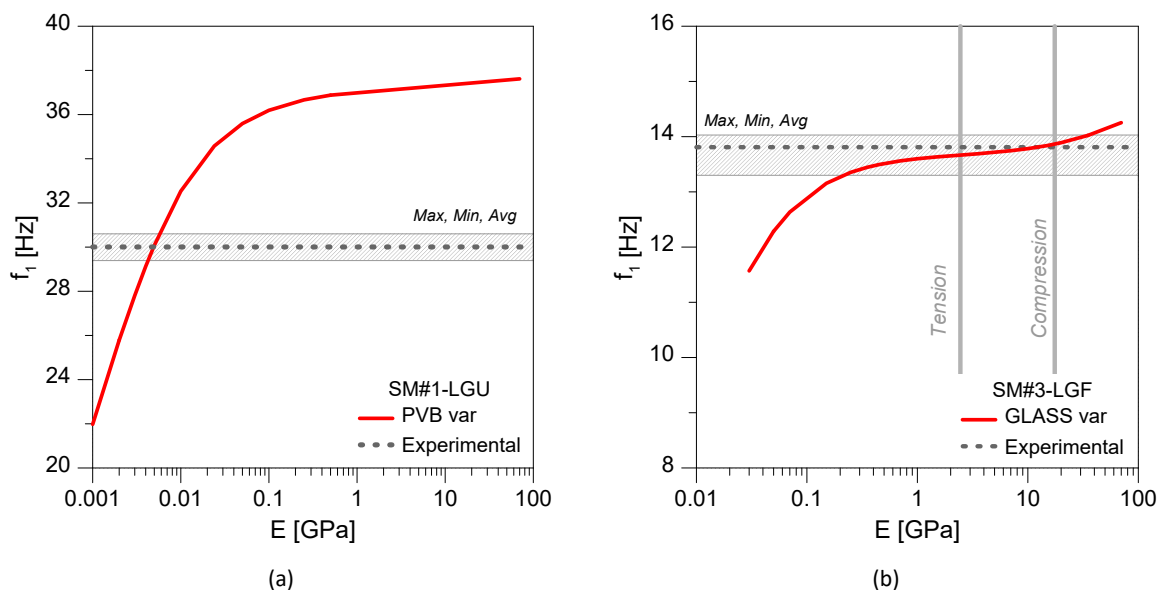


Fig. 10: Material characterization based on FE model updating:
 (a) interlayer stiffness for SM#1-LGU system and (b) fractured glass layer characterization for SM#3-LGF module.

More in detail, Figure 10 (a) shows the effect of PVB stiffness on the fundamental vibration frequency of SM#1-LGU module. Compared to the average experimental vibration frequency (with evidence of experimental range from a total of 9 signals), it can be seen that the best match is found for E modulus for PVB foils in the order of ≈ 4 -5 MPa. Worth to note that the so calculated equivalent E modulus is in the same order of magnitude of the study reported in (Bedon 2019a, Bedon & Noè 2021), where part of the Aquileia walkway panels have been experimentally investigated with a similar approach ($E = 4$ MPa the proposed equivalent modulus). The experimental study carried out by El-Sisi et al. (2020) on small-scale aged PVB samples under static and dynamic loads confirmed that aged specimens (8-year laboratory ageing protocol) are characterized by bi-linear constitutive response under high strain rates, but a strong decrease in stiffness and overall dynamic parameters, including energy absorption.

In Figure 10 (b), curve fitting is proposed for the SM#3-LGF module in which the degradation of PVB foils acts in combination with glass fracture for the top LG layer (Figure 2). The parametric FE analysis shows in this case that the best match of experimentally derived vibration frequency for the system is in the order of 15 GPa for the fractured glass layer, and this finding is in close correlation with the compressive fractured glass modulus calibrated in (Kozłowski 2019).

5. Residual structural capacity

5.1. Measure of mechanical degradation

The analysis of structural performances under quasi-static equivalent loads can offer robust feedback about the degradation progress and actual residual capacity for a given system. In the present study, the analysis of stress peaks and deflections was carried out with the support of FE numerical models adapted from previous frequency modal analyses (Figure 4). In doing so, input mechanical properties calibrated to experimental vibration frequencies were taken into account. The selected LG pedestrian systems were investigated under the effects of self-weight and a distributed accidental vertical load $Q_k = 4 \text{ kN/m}^2$. Further, the analysis was carried out for the pedestrian modules as in the “Current” situation and at “Time 0”, that is with a short-term elastic modulus for PVB and intact glass layers.

The so collected results are summarized in Table 5, where the percentage scatter of “initial” and “present” structural performances is also reported. In the analysis of performance indicators, moreover, maximum stress peaks are calculated:

- At the mid-span of short edges in free bending for SM#1-LGU system
- In the region of mechanical pint supports for SM#2-LGU and SM#3-LGF systems

Table 5: Structural performance analysis for the examined modular units (with single occupant, $M = 80 \text{ kg}$).

Sample	Vibration frequency [Hz]			ULS stress [MPa]			SLS deflection [mm]		
	Time 0	Current	Δ [%]	Time 0	Current	Δ [%]	Time 0	Current	Δ [%]
SM#1-LGU	34.6	30	-13.3	4.31	5.27	+22.2	1.16	1.76	+51.7
SM#2-LGU	21.2	15.05	-28.3	17.28 (point-fixing)	20.01	+15.8	4.11	6.10	+48.4
				6.29 (centre)	7.69	+18.2			
SM#3-LGF	21.2	13.8	-34.9	17.28 (point-fixing)	26.55	+53.64	4.11	6.28	+52.8
				6.29 (centre)	4.29	-31.8			

From Table 5, some useful parameters can be easily derived to quantify the actual capacity due to long-term effects and unfavourable operational conditions. In terms of vibration frequency of the occupied modules, for example, it can be seen that the SM#1-LGU system with minimum geometric slenderness and relatively short bending span is less affected by mechanical degradation of PVB foils, compared to the others. In contrary, the SM#3-LGF system affected by the additional fracture of glass show the maximum frequency decrease.

As far as the principal ULS stress peaks in glass are taken into account, Table 5 shows a rather balanced variation for SM#1-LGU and SM#2-LGU solutions. Conversely, the partial glass fracture in SM#3-LGF system gives clear evidence of more pronounced stiffness degradation, as a direct result of the fractured glass layer in compression. The analysis of SLS deflections, finally, shows rather comparable modifications for all the three examined systems, either under different geometrical and mechanical properties. In this sense, the analysis of deflection only may not be able to capture the actual damage scenario for a given in-service LG pedestrian system, while more robust feedback can be derived from the frequency analysis and stress analysis in glass. On the other side, all the examined performance indicators need the support of field experimental measurements and a further assessment based on accurate FE numerical models.

5.2. Safety check

As far as the design parameters from (CNR-DT 210/2013) or other design standards are taken into account, the parametric results in Table 5 can be further addressed towards design conditions.

More precisely, the limit SLS deflection should not exceed the value (2-edge linear supports for LG plates):

$$u_{lim} = \min \left\{ \begin{array}{l} 50 \text{ mm} \\ \frac{L_{min}}{100} \end{array} \right. \quad (12)$$

that is $u_{lim} = 5.1$ mm for SM#1-LGU and $u_{lim} = 13.5$ mm for SM#2-LGU and SM#3-LGF respectively.

Regarding the maximum ULS stress values in glass, the comparison is carried out towards the design strength as in CNR-DT 210/2013, where it is assumed that:

$$f_{g;d} = f_{g;d,b} + f_{g;d,p} = \frac{k_{mod}k_{ed}k_{sf}\lambda_g A \lambda_{gl} f_{g;k}}{R_M \gamma_M} + \frac{k'_{ed} k_v (f_{b;k} - f_{g;k})}{R_{M,v} \gamma_{M,v}} \quad (13)$$

with $f_{g;d,p} > 0$ for pre-stressed glass and:

$$k_{mod} = 0.585 \cdot t_L^{-1/16} \quad (14)$$

while the other coefficients and safety factors are defined in (CNR-DT 210/2013). The resistance verification notoriously requires that the stress effects of a given design action do not exceed the capacity of the system, that is:

$$\sigma_{max} \leq f_{g;d} \quad (15)$$

The application of Equation (15) to the examined in-service systems in ULS design conditions, with $k_{mod} = 0.78$, resulted in strength values in the order of ≈ 60 MPa at the edges and ≈ 74 MPa in the centre of LG panels. The so-derived ULS stress-to-strength and SLS deformation-to-deflection limit results are summarized in Table 6.

Table 6: Safety check for ULS stress and SLS deformation accounting for degradation phenomena.

Sample	ULS stress ratio			SLS deflection ratio		
	Time 0	Current	SAFE (≤ 1)	Time 0	Current	SAFE (≤ 1)
SM#1-LGU	0.071	0.087	Yes	0.22	0.35	Yes
SM#2-LGU	0.29	0.34	Yes	0.31	0.45	Yes
SM#3-LGF	0.29	0.45	Yes	0.31	0.47	Yes

More specifically, it can be seen that the ULS stress analysis is largely satisfied for the SM#1-LGU system with relatively short bending span and small geometric slenderness. Besides, the SLS deflection limit, still satisfied, is the governing parameter for overall safety check.

For the SM#2-LGU module, the SLS deflection check is also associated to major structural effects due to occupants, while a less pronounced modification of control parameters can be noticed for ULS stress peaks. Finally, for the SM#3-LGF system affected by partial glass fracture, it is possible to see a rather uniform safety check for ULS stress and SLS deformation values.

Overall, the examined systems are “safe” for occupants but give evidence of marked loss of structural capacity, compared to “Time 0” design performances. In this sense, such a kind of procedure can offer a robust and concise damage index for monitoring or retrofit interventions. Furthermore, in presence of intermittent field experimental measures of vibration frequencies, can be cyclically carried out to follow the progress of material deterioration from the original installation apart.

6. Summary and conclusions

Knowledge of actual mechanical properties and residual capacity for in-service laminated glass (LG) structures is of utmost importance, especially for systems characterized by direct interaction with occupants. While in certain conditions damage can be visually detected, however, there are situations in which the in-service structure is potentially unsafe (due to unfavourable operational conditions, material degradations, etc.) without visual defects. In this sense, a protocol to rapidly assess the structural safety and estimate the residual capacity of these systems is crucial. In this paper, the attention was focused on 3 different LG pedestrian modular units belonging to 2 different in-service systems in Italy. The attention was given to the assessment of potential and limits of different procedures to detect potential risk and damage phenomena, without the support of dedicated laboratory instruments and setup configurations.

In terms of vibration assessment, the study gave evidence that:

- The estimation of fundamental vibration frequency is a first but not sufficient step for safety characterization. LG pedestrian systems are often characterized by relatively high fundamental frequency, but an overall dynamic performance which is severely affected by the mass of occupants.
- In this sense, fast intermittent field measures based on single sensor and OMA techniques would allow to collect comparative data for an efficient and rapid check of mechanical modifications in the structure, based on vibration frequency only.
- Most of existing conventional methods are not specific for LG pedestrian systems, and thus calibrated to different constructional typologies. In this sense, a direct comparison of field experimental measures may result in not meaningful conclusions for safety check purposes.
- Damping estimates from field experimental signals is often affected by various parameters, but could reveal some marks of damage severity by comparison of similar slab units.
- The analysis of performance indicators (acceleration peak, RMS acceleration, RMS velocity) can suggest the potential presence of damage and / or material degradation, as it was shown for the SM#3-LGF unit affected by glass fracture.

In terms of stress and deformation checks, it was shown that:

- Long-term phenomena and material degradation can induce severe modifications in structural performances, compared to “Time 0” design conditions.
- The comparison of “Current” and “Time 0” stress and deflection performances offers strong feedback, especially when vibration frequency modifications are unknown.

In such an overall procedure, the use of a single sensor for field measurements gives a multitude of parameters, but necessarily needs robust knowledge for experimental setup and interpretation of data. Similarly, the availability of field experimental measures is meaningful especially when combined to refined Finite Element numerical models able to quantify the long-term / damage effects, compared to state-of-art condition.

Acknowledgements

Seretti Vetroarchitetture is acknowledged for giving access to the SM#1-LGU system during retrofit interventions (San Giorgio di Nogaro (UD), Italy). So.Co.Ba. is also acknowledged for facilitating the field experimental investigation on SM#2-LGU and SM#3-LGF systems. (Aquileia (UD), Italy).

Conflict of interest

The authors declare there is no conflict of interest with the publication of this manuscript.

References

- Andreozzi, L., Briccoli Bati, S., Fagone, M., Ranocchiai, G., Zulli, F., Weathering action on thermo-viscoelastic properties of polymer interlayers for laminated glass. *Constr. Build. Mater.* (2015), 98. 757–766
- Baggio, C., Bernardini, A., Colozza, R., Corazza, L., Della Bella, M., Di Pasquale, G., Dolce, M., Goretti, A., Martinelli, A., Orsini, G., Papa, F., Zuccaro, G., Field Manual for post-earthquake damage and safety assessment and short term countermeasures (AeDES), Report EUR 22868 EN (2007) – Joint Research Centre – Institute for the Protection and Security of the Citizen, Editors: Artur V. PINTO, Fabio TAUCER, ISSN 1018-5593
- Bedon, C.: Diagnostic analysis and dynamic identification of a glass suspension footbridge via on-site vibration experiments and FE numerical modelling. *Composite Structures* (2019a), 216: 366-378
- Bedon, C.: Issues on the Vibration Analysis of In-Service Laminated Glass Structures: Analytical, Experimental and Numerical Investigations on Delaminated Beams. *Appl. Sci.* (2019b), 9: 3928, <https://doi.org/10.3390/app9183928>
- Bedon, C.: Experimental investigation on vibration sensitivity of an indoor glass footbridge to walking conditions. *J Build Eng* (2020), 29: 101195
- Bedon, C., Noè, S.: Post-Breakage Vibration Frequency Analysis of In-Service Pedestrian Laminated Glass Modular Units. *Vibration* (2021), 4(4): 836-852, <https://doi.org/10.3390/vibration4040047>
- Bedon, C., Fasan, M., Reliability of field experiments, analytical methods and pedestrian's perception scales for the vibration serviceability assessment of an in-service glass walkway. *Applied Sciences* (2019), 9(9): 1936; <https://doi.org/10.3390/app9091936>
- Bedon, C., Fasan, M., Amadio, C., Vibration analysis and dynamic characterization of structural glass element with different restraints based on operational modal analysis. *Buildings* (2019), 9: 13
- Bedon, C., Mattei, S., Facial Expression-Based Experimental Analysis of Human Reactions and Psychological Comfort on Glass Structures in Buildings. *Buildings* (2021), 11: 20, <https://doi.org/10.3390/buildings11050204>
- Bedon, C., Bergamo, E., Izzi, M., Noè, S., Prototyping and validation of MEMS accelerometers for structural health monitoring—The case study of the Pietratagliata cable-stayed bridge. *J. Sens. Actuator Netw.* (2018), 7, doi:10.3390/jsan7030030

- Busca, G., Cappellini, A., Manzoni, S., Tarabini, M., Vanali, M., Quantification of changes in modal parameters due to the presence of passive people on a slender structure. *J. Sound Vib.* (2014), 333: 5641-5652
- Cao, M.S., Sha, G.G., Gao, Y.F., Ostachowicz, W., Structural damage identification using damping: a compendium of uses and features, *Smart Materials and Structures* (2017), 26(4): 043001
- Clough, R.W., Penzien, J., *Dynamics of Structures*; McGraw-Hill: New York, NY, USA (1993) ISBN 0-07-011394-7
- CNR-DT 210/2013, Istruzioni Per la Progettazione, L'esecuzione ed il Controllo di Costruzioni con Elementi Strutturali di Vetro; National Research Council of Italy (CNR): Roma, Italy, 2013. (In Italian)
- Dimarogonas, A.D., Vibration of cracked structures: A state of the art review. *Eng. Fract. Mech.* (1996), 55: 831-857
- El-Sisi, A., Newberry, M., Knight, J., Salim, H., Nawar, M., Static and high strain rate behavior of aged virgin PVB. *J Polym Res* 29, 39 (2022). <https://doi.org/10.1007/s10965-021-02876-5>
- Feldmann, M., Heinemeyer, C., Butz, C., Caetano, E., Cunha, A., Galanti, F., Goldack, A., Hechler, O., Hicks, S., Keil, A., Lukic, M., Obiala, R., Schlaich, M., Sedlacek, G., Smith, A., Waarts, P., Design of floor structures for human induced vibrations (2009), EUR 24084 EN. Luxembourg (Luxembourg): Publications Office of the European Union; 2009. JRC55118
- Kozłowski, M., Experimental and numerical assessment of structural behaviour of glass balustrade subjected to soft body impact. *Compos. Struct.* (2019), 229: 111380
- Galuppi, L., Royer-Carfagni, G., Effective thickness of laminated glass beams: new expression via a variational approach. *Engineering Structures* (2012), 38: 53-67
- Harirchian, E., Lahmer, T., Buddhiraju, S., Mohammad, K., Mosavi, A., Earthquake Safety Assessment of Buildings through Rapid Visual Screening. *Buildings* (2020), 10: 51, <https://doi.org/10.3390/buildings10030051>
- Huang, Z., Xie, M., Du, J.Z.Y.M., Song, H.-K., Rapid evaluation of safety-state in hidden-frame supported glass curtain walls using remote vibration measurements. *J. Build. Eng.* (2018), 19: 91-97
- ISO 10137:2007, Bases for design of structures -Serviceability of buildings and walkways against vibrations, International Organisation for Standardization (ISO)
- Limongelli, M.P., Manoach, E., Quqa, S., Giordano, P.F., Bhowmik, B., Pakrashi, V., Cigada, A., Vibration Response-Based Damage Detection. In *Structural Health Monitoring Damage Detection Systems for Aerospace*; Springer Aerospace Technology, Switzerland (2021)
- Ministry of Business, Innovation and Employment (MBIE). Field Guide: Rapid post disaster building usability assessment – earthquake (2014, 1st edition), ISBN: 978-0-478-41794-4 (Print) / 978-0-478-41797-5 (Online)
- Sedlacek, G., Heinemeyer, C., Butz, C., Völling, B., Waarts, P., Duin, F., Hicks, S., Devine, P., Demarco, T., Generalisation of criteria for floor vibrations for industrial, office, residential and public building and gymnastic halls (2006), Report number: EUR-21972-EN (Luxembourg: European Commission)
- Simulia, ABAQUS. ABAQUS Computer Software, Dassault Systèmes: Providence, RI, USA, 2021
- Stepinac, M., Kisicek, T., Renić, T., Hafner, I., Bedon, C., Methods for the Assessment of Critical Properties in Existing Masonry Structures under Seismic Loads—The ARES Project. *Appl. Sci.* (2020), 10: 1576, <https://doi.org/10.3390/app10051576>
- Zemanova, A., Zeman, J., Janda, T., Schmidt, J., Sejnoha M., On modal analysis of laminated glass: usability of simplified methods and Enhanced Effective Thickness. *Composites Part B* (2018), 151: 92-105

Platinum Sponsors

The Eastman logo, consisting of the word 'EASTMAN' in a bold, red, sans-serif font.

Gold Sponsors

The Bellapart logo, featuring the word 'Bellapart' in a bold, blue, sans-serif font.The kuraray logo, featuring the word 'kuraray' in a blue, lowercase, sans-serif font.The Trosifol logo, featuring the word 'Trosifol' in a black, sans-serif font with a registered trademark symbol.The SentryGlas logo, featuring the word 'SentryGlas' in a black, sans-serif font with a registered trademark symbol.The sedak logo, featuring the word 'sedak' in a bold, black, lowercase, sans-serif font.

Silver Sponsors

The octatube logo, featuring the word 'octatube' in a bold, italicized, black, sans-serif font.The vitroplena structural glass solutions logo, featuring a blue stylized 'v' icon followed by the text 'vitroplena structural glass solutions' in a black, sans-serif font.

Organising Partners

The TU/e logo, featuring the text 'TU/e' in a bold, red, sans-serif font.The TU Delft logo, featuring a black stylized flame icon above the text 'TU Delft' in a bold, black, sans-serif font.